

P. MRVA*, D. KOTTFFER**, Ł. KACZMAREK***

EFFECT OF SHOT PEENING AND NiAl COATING ON FATIGUE LIMIT OF Mg-Al-Zn-Mn ALLOY

WPLYW PARAMETRÓW ŚRUTOWANIA ORAZ OSADZENIA POWŁOKI NiAl NA WŁAŚCIWOŚCI ZMĘCZENIOWE STOPU Mg-Al-Zn-Mn

The paper deals with an influence of cyclic load on fatigue limit of the Mg-Al-Zn-Mn alloy without or with the NiAl coating. The fatigue limit was determined for the following three types of specimens of the Mg-Al-Zn-Mn alloy: (1) fine-turned specimens; (2) fine-turned specimens with an application of the shot peening process; (3) fine-turned and shot-peened specimens with the NiAl coating deposited by the thermal spraying technique. A standard measurement of the fatigue limit was used for the analytical determination of the Wohler curves (S-N curves). The Wohler curves for the specimens (1) and (3) were in agreement with those presented in literature. The specimens (2) exhibited a lower value of the fatigue limit compared with that of the specimens (1), although the increase of the fatigue limit of the specimens (2) was expected due to the presence of the application of the shot peening process. An analysis of reasons of the decrease of the fatigue limit of the specimens (2) is presented.

Keywords: fatigue limit, fatigue strength, high cycle fatigue, S-N curves, shot peening

W niniejszym artykule przedstawiono wyniki badań obciążenia cyklicznego na wytrzymałość zmęczeniową na zginanie stopu Mg-Al-Zn-Mn bez lub z naniesioną powłoką NiAl. Badaniu poddano trzy typy próbek wykonanych ze stopu Mg-Al-Zn-Mn: (1) próbki bez modyfikacji powierzchniowej; (2) próbki poddane procesowi śrutowania; (3) próbki poddane procesowi śrutowania wraz z późniejszym naniesieniem powłoki NiAl metodą natryskiwania cieplnego. Uzyskane wyniki zobrazowane na krzywych Wohler'a dla próbek grupy (1) i (3) są zgodne z danymi zawartymi w literaturze. W przypadku natomiast próbek grupy (2) mimo, iż zostały poddane śrutowaniu charakteryzują się niższą wytrzymałością zmęczeniową w porównaniu do próbek nie poddanych modyfikacji powierzchniowej – grupa (1). W niniejszym artykule podjęto również próbę wyjaśnienia obniżenia się właściwości zmęczeniowych próbek poddanych śrutowaniu.

1. Introduction

Nowadays a special interest is focused on the development of high strength and light weight alloys based on aluminium or magnesium for applications in aerospace and automobile industry mainly due to increase of range and/or load carrying capacity, decrease of fuel consumption of vehicles [1÷5]. Magnesium alloys are frequently used for low stress applications (e.g. wheels, automotive bodies), and less frequently, mainly due to mechanical limits for mechanically loaded structural components (e.g. transmission housings, automotive axles) [6,7].

In case of aircraft industry the problem of renovation of aerial components made from Mg alloys is actual and can be realized by deposition of thin coatings (few micrometers) with required properties (e.g. abra-

sion resistance, fatigue behavior, degradation parameter D [8], adhesion [9], etc.). Coatings are deposited mainly by: PVD [8÷10], CVD, PE CVD techniques, by thermal spraying technique – with plasma stimulated arc or by electron beams to produce functionally graded substrate layers using cored wire electrodes [6,11]. However, during deposited process could forming oxide phases what could have disastrous failure during operation of aerial components particularly exposed to high-cycle fatigue. Other materials used for engine blades are Ni superalloys with protective Al-Si coatings [11,12]. Degradation mechanisms of structures and coatings are functions of engine operating conditions, engine mechanical design and utilized materials. They all together determine the life-time of the engine [13].

* DEPARTMENT OF AVIATION ENGINEERING, FACULTY OF AERONAUTICS, TECHNICAL UNIVERSITY IN KOŠICE, RAMPOVA 7, 041 21 KOŠICE, SLOVAKIA

** DEPARTMENT OF TECHNOLOGIES AND MATERIALS, FACULTY OF MECHANICAL ENGINEERING, TECHNICAL UNIVERSITY IN KOŠICE, MÁSIARSKA 74, 040 01 KOŠICE

*** INSTITUTE OF MATERIAL SCIENCE AND ENGINEERING, TECHNICAL UNIVERSITY OF ŁÓDŹ, 90-924 ŁÓDŹ, 1/15 STEFANOWSKIEGO STR., POLAND

The high-cycle fatigue (HCF) behavior of Mg alloys (Mg–Zn–Y–Zr) is strongly affected by the loading spectrum and heat treatment process [14].

Rajasekaran et al. studied fatigue properties of Al–Mg–Si alloy treated by microarc oxidation (MAO) technique. While uncoated substrate could withstand a maximum cyclic stress of 160 MPa for 2×10^6 cycles without failure, 40 μm thick coated specimen failed after 2×10^5 cycles and 100 μm thick coated specimen failed after 1.1×10^5 cycles [15]. Several researchers studied the tribological properties of MAO coatings on Al, Ti, Mg base and their alloys under different conditions and proved that MAO coating provides excellent adhesion with the substrate and has improved wear resistance, corrosion resistance, chemical stability, high temperature shock resistance, etc. [15–23].

Lonyuk et al used electroless technique for the deposition of the electroless nickel-phosphorous (NiP) coatings with the thickness $17 \pm 1 \mu\text{m}$. The results of the fatigue test indicated an increased fatigue life of the coated aluminium alloy up to 150% (uncoated substrate tested at 170 MPa and fractured after 6×10^6 cycles, substrate with electroless NiP coating tested at 200 MPa and fractured after 2×10^6 cycles) [24].

Yerokhin et al. studied effect of Keronite coatings (by Kerotite Ltd. improved plasma electrolytic oxidation – PEO – technique) on fatigue behaviour of Mg–Al–Zn–Mn alloy rod (2% Al, 1% Zn, 0.2% Mn, Mg – balance). This coating reduced fatigue limit of the Mg–Al–Zn–Mn alloy following: from 85 MPa (surface without coating) to 81 MPa, 6.5×10^5 cycles (a coating with thickness $7 \mu\text{m}$), to 77 MPa (a coating with thickness $15 \mu\text{m}$) [25]. The results of fatigue tests demonstrate that Keronite coatings may cause no more than a 10% reduction in fatigue limit of the Mg alloy [25].

The mechanism of oxide layer formation during PEO represents a complex combination of conventional anodic oxide film growth with plasma enhanced surface oxidation in ‘micro-arc’ discharge regions, leading to fusing and recrystallisation of the oxide film [26]. However, an improved PEO method, utilising a pulsed bipolar current, has recently been developed and made commercially available by Keronite Ltd.

The studied material is Mg alloy which is used for wheels production of some militar aircrafts. This aircraft parts are working in conditions of various dynamic loads. The typical picture of the wear of aircraft parts are cracks. This one are the result of the cyclical fatigue of the material. This one have the relevant influence on-to lifetime of aircraft parts and this is cause to put out of service [27,28]. The research of Mg alloys is led to determination complex properties [29].

Aim for study was chosen the determination of influence of cyclical loading onto fatigue limit of Mg–Al–Zn–Mn alloy three specimen surfaces: without mechanical pretreatment (fine turned surface), with shot peened surface and with thermal sprayed NiAl coating.

2. Preparation of specimens and experimental procedure

Fatigue test specimens (STN 42 4911) with ends diameter of 10 mm, minimum gauge length diameter of 6 mm and total length of 80 mm (Fig.1) were made from a magnesium alloy rod (8.5% Al, 0.5% Zn, 0.3% Mn, 90.7% Mg – balance) [30]. The specimens were shaped by fine turning to the required dimensions, to achieve a surface roughness of approximately $R_a = 0.05 \mu\text{m}$. Next the specimens were shot peened by apparatus HUNZIKER to a surface roughness of approximately $R_a = 5.5 \mu\text{m}$. For shot peening was used electrocorundum No. 30, brown with grain size from 500 to $630 \mu\text{m}$, the airpressure from 0.3 to 0.4 MPa. Mechanical features are showed in Table 1.

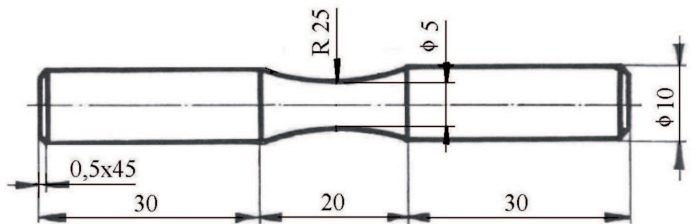


Fig. 1. Specimen shape used in the present investigation

TABLE 1
Mechanical properties of Mg–Al–Zn–Mn alloy

	R_m [MPa]	R_e [MPa]	A_5 [%]
Mg alloy	250	90	8,0

The NiAl coating was deposited by thermal spraying technique, by the apparatus SCHULZER METCO. Parameters of thermal spraying process were as follows: the plasma current $I_p = 450 \text{ A}$; the plasma voltage $U_p = 60 \text{ V}$; the capacity of the plasma gas $Q = 0.033 \text{ m}^3 \text{ min}^{-1}$; the gas compound 78% Ar + 22% H_2 ; the specimen distance to output of a nozzle $l = 140 \text{ mm}$; the gas transportation capacity $\text{Ar} = 0.0021 \text{ m}^3 \cdot \text{min}^{-1}$. The compound of deposited material is NiAl 80% Ni, 20% Al, and the grain diameter is $d_z = 40\text{--}45 \mu\text{m}$. The coating thickness was $h = 500\text{--}600 \mu\text{m}$, the coating roughness was $R_a = 12\text{--}14 \mu\text{m}$, the coating porosity was 2–3%.

The fatigue test, i.e. the cyclical rotary bending ($R=-0.1$), was made by rotary bending machine SCHENK at temperature 18 to 20°C, frequency 100 cycles. s^{-1} .

The S-N curves were created by 25 specimens (Fig. 2). Values of fatigue limit were investigated in the failure moment of investigated specimens. Values of the fatigue limit of Mg-Al-Zn-Mn alloy with shot peened surface were determined at 10^8 cycles.

Stresses were calculate by the equation

$$\sigma = \sigma_a - \frac{W_{6,74}}{W_{sk}}, \quad (1)$$

where σ_a is a start stress [MPa], $W_{6,74}$ is a module of a standard specimen [cm^3], and W_{sk} is a module of a specimen [cm^3].

The fracture line and fracture surfaces have been studied by fractographic methods.

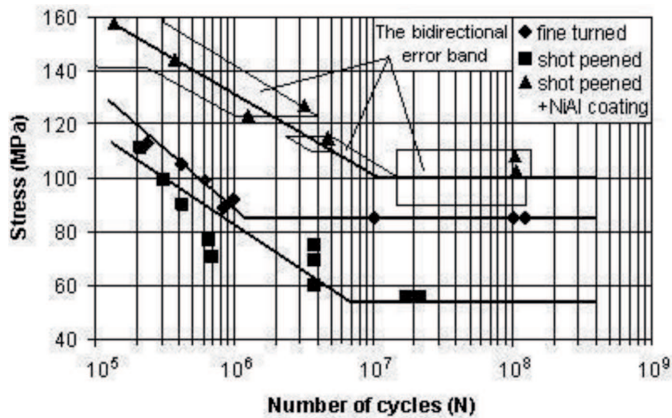


Fig. 2. S-N curves of the tested specimens (Mg-Al-Zn-Mn alloy): with fine turned surface, with the shot peened surface, with the shot peened surface and NiAl coating

3. Results and discussion

The S-N diagram is shown in Fig. 2. It reveals that the shot peening process to create a layer with thickness of approx. $50 \mu m$ (see Fig. 3) reduced the fatigue limit from 85 MPa to 54 MPa, where the surface layer was strengthened by the shot peening process. Subsequently, prolongation of the shot peening process resulted in the decrease of plasticity, significant strengthening, and high roughness of the surface layer, the last characterized by big values of R_{max} . The big values thus were a reason of high values of the surface stresses acting on the shot-peened surface. The surface stresses induced surface cracks with critical size to be consequently a reason of the initiation of a fatigue crack during the fatigue test.

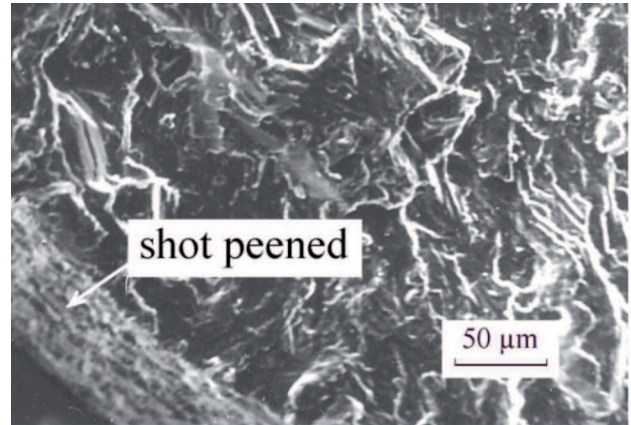


Fig. 3. Fatigue fracture of the specimen with shot peened surface with thickness of approx. $50 \mu m$

The fatigue limit of the fine-turned specimens at 10^6 cycles is higher (approx. 7%) compared with that of shot peened specimens (Fig. 2).

Considering Fig. 2, the NiAl thermal sprayed coating exhibited an influence on the fatigue limit increasing from 54 MPa to 100 MPa. The fatigue limit of the specimens with NiAl coating is influenced by a sign and the distribution of surface stresses originating during the deposition proces in the surface coating [31]. The surface stresses in thermal sprayed coatings are represented by thermal stresses [32,33] originating due to the difference $\alpha_{Mg-alloy} - \alpha_{NiAl} > 0$ [34] in thermal expansion coefficients of $\alpha_{Mg-alloy}$ and α_{NiAl} for Mg-Al-Zn-Mn and NiAl, respectively. In case of the NiAl-(Mg-Al-Zn-Mn) system, the difference is sufficient regarding the investigation of an influence of the thermal stresses to the fatigue limit. Due to $\alpha_{Mg-alloy} - \alpha_{NiAl} > 0$, the thermal stresses in NiAl are compressive, and might be thus assumed to represent the prevention from the initiation of the fatigue crack.

Additionally, microstructure of the NiAl thermal spraying coating might be assumed to be a reason of a change of a direction of the fatigue crack from the vertical direction to the parallel one regarding a surface of the specimen (Fig. 4). Other reasons influencing the fatigue limit are inconstant temperature of the specimen surface, and its plastic deformation to originate during the shot peening process followed by the thermal spraying.

The overall fracture surfaces of specimens are shown in Fig. 3, 5 a-c and 6.

The roughness of the coated specimen surfaces is $R_a=5,75\mu m$. Cracks in the surface of specimens was occur on the polished cross-section (Fig. 4). The structure of fatigue fractures was seen by the scanning microscope Jeol JSM-U3. The structure of fractures of the specimen with fine turned surface and of the specimen with shot peened surface show any differenceses.

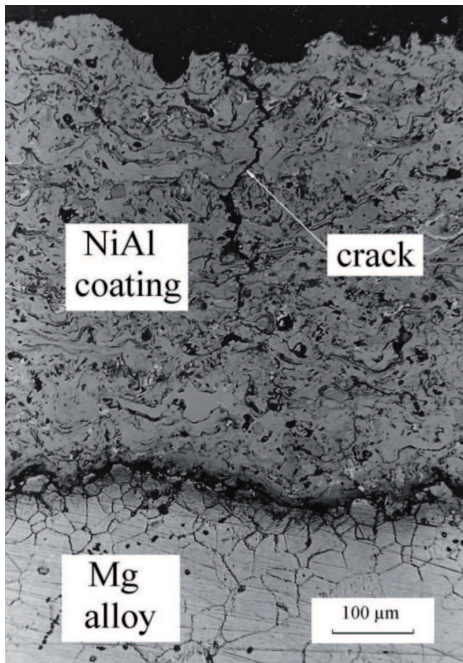


Fig. 4. Optical image of polished cross-section of specimen – Mg alloy with NiAl coating subjected to the fatigue testing

The structure at different magnifications of the fracture of the specimen with NiAl coating shows different morphological porous pattern (Fig. 5a÷c). The chemical design of porous phases was determined by DTA apparatus Tracor-Northern TN-2000: 90%Mg, 0.89%Al, 0.33%P, 1.24%Fe, 4.3%Ni, 2.67%Zn. The matrix of the fracture has the following chemical composition: 89.46%Mg, 3.85%Ni, 4.88%Zn, 2.06%Fe. Chosen patterns are evoked by casting process of the liquid alloy to the skillet. The endurance limit of studied material of three surfaces (fine turned, shot peened and with NiAl thermal sprayed coating) was determined by linear dependence of logarithm of cycles number lgN on stresses σ by equations [35]

$$lgN = a + b \cdot \sigma, \quad (2)$$

where a , b are unknown parameters.

The equation (2) can be derived as

$$\hat{N} = \exp(abR). \quad (3)$$

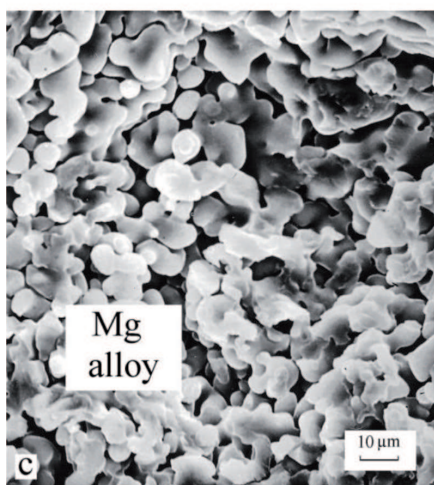
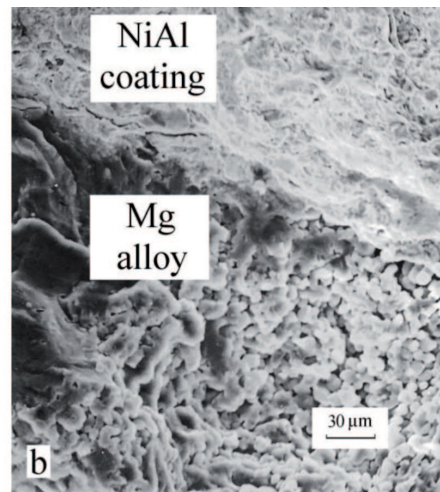
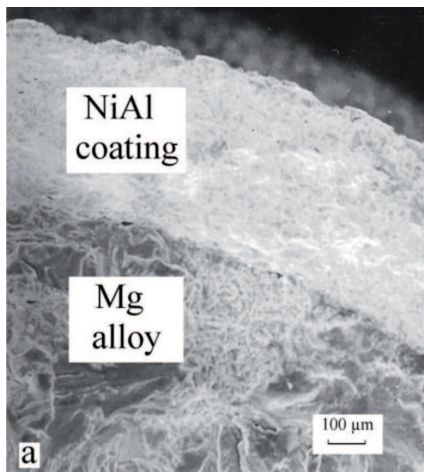


Fig. 5. Fatigue fracture of the Mg alloy with NiAl coating

The unknown parameters a , b determined by results of fatigue tests by the method of the least squares method from following equations

$$a = \frac{1}{n} \sum_{i=1}^n \lg N_i - b \cdot \frac{1}{n} \sum_{i=1}^n \sigma_i, \quad (4)$$

$$b = \frac{n \sum_{i=1}^n \lg N_i \sigma_i - \sum_{i=1}^n \sigma_i \cdot \sum_{i=1}^n \lg N_i}{n \sum_{i=1}^n \sigma_i^2 - \left(\sum_{i=1}^n \sigma_i \right)^2}, \quad (5)$$

$$\bar{\sigma} = \frac{1}{n} \sum_{i=1}^n \sigma_i, \quad (6)$$

$$l\hat{g}N = \frac{1}{n} \sum_{i=1}^n \lg N_i. \quad (7)$$

With the estimation of the general dispersion ($\lg N$) is the selective dispersion calculated by the following equation

$$S^2 \{ \lg N \} = \frac{1}{2n} \sum_{i=1}^n \left[\lg N_i - l\hat{g}N(a, b, \sigma_i) \right]^2 = \frac{1}{2n} \left[\sum_{i=1}^n (\lg N_i)^2 - a \sum_{i=1}^n \lg N_i - b \sum_{i=1}^n N_i \sigma_i \right]. \quad (8)$$

This dispersion shows the tolerance rate of measured values of test by submitted dependency.

The bidirectional error band (Fig.2) of mathematical expectation of value $E(\lg N/\sigma)$ can be determined from followed mathematical relation

$$\lg \hat{N}(a, b, \sigma) - k(\sigma) \leq E[\lg(N/\sigma)] \leq \lg \hat{N}(a, b, \sigma) + k(\sigma), \quad (9)$$

$$k(\sigma) = t_{\alpha}(\gamma) \cdot S(\lg N) \cdot \left[\frac{1}{n} + \frac{n \cdot (\sigma - \bar{\sigma})^2}{n \cdot \sum_{i=1}^n \sigma_i^2 - \left(\sum_{i=1}^n \sigma_i \right)^2} \right]^{1/2}, \quad (10)$$

where $t_{\alpha}(\gamma)$ is quantile of error band of the Student's cumulative distribution function for the error band $\alpha=0,1$ ($\alpha=0,05$ for aircraft parts) and for degrees of freedom $\gamma=n-2$.

The error band growth for different σ with the value growth of $(\sigma - \bar{\sigma})$. Results and calculated parameters of equations are in Table 2.

It can be observed that measured values are in the bidirectional error band (Fig.2).

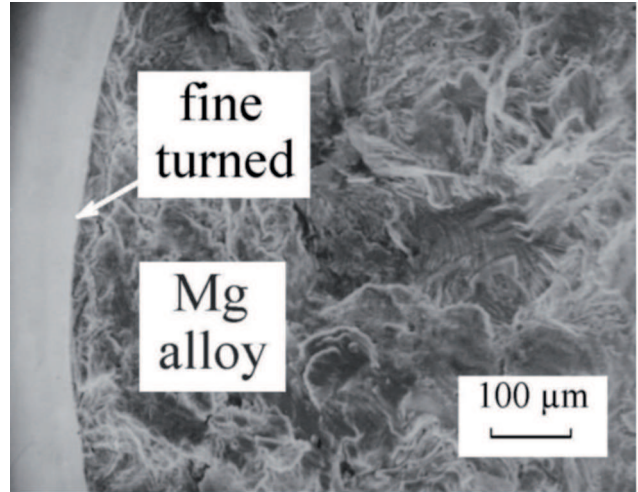


Fig. 6. Fatigue fracture of the Mg alloy without coating, fine turned surface

TABLE 2

Coefficients and equations of S-N curves of investigated Mg specimens

specimen surface	a	b	$l\hat{g}N = a + b \cdot \sigma$
fine turned	14.0687	-0.0807	$l\hat{g}N = 14.0687 - 0.0807 \cdot \sigma$
shot peened	8.7358	-0.0318	$l\hat{g}N = 807358 - 0.0318 \cdot \sigma$
with NiAl coating	12.3799	-0.0471	$l\hat{g}N = 12.3799 - 0.0471 \cdot \sigma$

It can be observed that shot peening creates the pressure residual stresses onto coating of substrate. This pressure residual stresses have low effect onto fatigue limit. The surface roughness effects on the endurance limit, especially. The big values of the depth (R_{max}) and the little radius of the depth cause high concentration of the stresses on shot peened surface of the specimen. This concentration effects more onto the fatigue limit as pressure stresses. It can be written that the convenient treatment of the surface before coating deposition (for example by shot peening) enlarges values of endurance limit of Mg-Al-Zn-Mn alloys. Next it can be predicted that the surface is deformed by a process of the coating deposition. It reduced the concentration of stresses.

4. Conclusions

In the cycle fatigue regime (10^5-10^8 cycles), influence of the fine turned surface, shot peening and thermal sprayed NiAl coating for the forged Mg-Al-Zn-Mn alloy has been investigated and the main results are the following:

- The fatigue limit of uncoated fine turned specimen was 85MPa.
- Shot peening of specimens of evaluated Mg-Al-Zn-Mn alloy by electrocorundum reduced

fatigue limit from 85 to 54,5MPa. In this case the shot peening evoked high roughness R_{max} , concentration of surface stresses, and nuclei of cracks. The nuclei of cracks are a reason of the initiation of the fatigue crack to reduce the fatigue limit.

- NiAl coating deposited on the shot peened surface properly distorted surface, reduced concentration of surface stresses and so enhanced the fatigue limit from 85 to 100MPa. The cycle frequency was 100Hz. The thickness of NiAl coating was 500 μ m.
- The microstructure of the NiAl thermal spraying coating might be assumed to be a reason of a change of a direction of the fatigue crack from the vertical direction to the parallel one regarding a surface of the specimen (Fig.4).

Acknowledgements

This work was financially supported by the Slovak Grant Agency under the grant VEGA 1/0378/08.

REFERENCES

- [1] Ł. Kaczmarek, P. Kula, J. Sawicki, S. Armand, T. Castro, P. Kruszyński, A. Rochel, Archives of Metallurgy and Materials **54**, 1199-1205 (2009).
- [2] D.H. Bae, S.H. Kim, D.H. Kim, W.T. Kim, Acta Mater. **50**, 2343 (2002).
- [3] L.L. Rokhlin, Archives of Metallurgy and Materials **52**, 5-11 (2007).
- [4] J. Adamiec, A. Kierzek, Archives of Metallurgy and Materials **55**, 69-78 (2010).
- [5] P. Skubisz, J. Sińczak, Archives of Metallurgy and Materials **52**, 329-336 (2007).
- [6] B. Wielage, A. Wank, H. Pokhmurska, S. Thiemer, Archives of Metallurgy and Materials **50**, 241-250 (2005).
- [7] H. Mayer, M. Papakyriacou, B. Zettl, S.E. Stanzl-Tschegg, Inter. J Fatig. **25**, 245 (2003).
- [8] M. Ferdinandy, F. Lofaj, J. Dúza, J. Ďurišin, Acta Metallurg. Slovaca **13**, 144 (2007).
- [9] M. Hagarová, I. Štěpánek, Metallic Materials **46** (3)165-172 (2008).
- [10] S. Pietrowski, Archives of Metallurgy and Materials **55**, 905-914 (2010).
- [11] J. Pokluda, M. Kianicová, Engineering Failure Analysis, **17**, 1389-1396 (2010).
- [12] M. Kianicová, Fireproof diffusive coating degradation in consequence of short-time operating temperature exceeding, PhD thesis, AD University in Trencin (2006).
- [13] M. Hetmanczyk, L. Swadzba, B. Mendala, J Achieve Mater Manuf Eng **24** (1), 372-81 (2007).
- [14] Z.-H. Liu, E.-H. Han, L. Liu, Mat. Sci. Eng. A **483-484**, 373 (2008).
- [15] B. Rajasekaran, G.S.S. Raman, S.V. Joshi, G. Sundararajan, Inr. J. Fatig. **30**, 1259 (2008).
- [16] P.A. Dearnley, J. Gummersbach, H. Weiss, A.A. Ogwu, T.J. Davies, Wear **225-229**, 127 (1999).
- [17] X. Shi-Gang, S. Li-Xin, Z. Rong-Gen, H. Xing-Fang, Surf. Coat. Tech. **199**, 184 (2005).
- [18] X. Shi-Gang, S. Li-Xin, Z. Rong-Gen, H. Xing-Fang, Mater. Chem. Phys. **97**, 132 (2006).
- [19] X. Nie, A. Leyland, H.W. Song, A.L. Yerokhin, S.J. Dowey, A. Matthews, Surf. Coat. Tech. **116-119**, 1055 (1999).
- [20] A.L. Yerokhin, X. Nie, A. Leyland, A. Matthews, Surf. Coat. Tech. **130**, 195 (2000).
- [21] W. Yaming, L. Tingquan, G. Lixin, J. Bailin, App. Surf. Sci. **252**, 8113 (2006).
- [22] R.L. Krishna, K.R.C. Somaraju, G. Sundararajan, Surf. Coat. Tech. **163-164**, 484 (2003).
- [23] R.L. Krishna, S.A. Purnima, G. Sundararajan, Wear **261**, 1095 (2006).
- [24] B. Lonyuk, I. Apachitei, J. Duszczyk, Scripta Mater. **57**, 783 (2007).
- [25] A.L. Yerokhin, A. Shatrov, V. Samsonov, P. Shashkov, A. Leyland, A. Matthews, Surf. Coat. Tech. **182**, 78 (2004).
- [26] A.L. Yerokhin, X. Nie, A. Leyland, A. Matthews, S.J. Dowey, Surf. Coat. Technol. **122**, 73 (1999).
- [27] P. Mrva, Research Report, Military Research Institute, Brno (1993).
- [28] P. Mrva, Research report, Research Institut of U.S. Steel, Kosice (1995).
- [29] M. Kuffová, MOSATT 2005, Proc. Int. Sci. Conf. Kosice, 269 (2005).
- [30] Wheel KT-92. Technical description of the wheel (1992).
- [31] V. Sedláček, Metall Surfaces and coatings. CVUT, Praha (1992).
- [32] L. Ceníga, J Mater Sci **38**, 3709 (2003).
- [33] L. Ceníga, Acta Metalurgica Slovaca **13**, 191 (2007).
- [34] P. Skočovský, O. Bokůvka, R. Konečná, E. Tillová, Materials Science for Mechanical Engineers, EDIS Technical University, Zilina, (2001).
- [35] STN EN 42 0363, Fatigue Tests of Metals, Technique of realization.